Taiwanese Journal of Obstetrics & Gynecology 55 (2016) 552–557

Contents lists available at ScienceDirect

Taiwanese Journal of Obstetrics & Gynecology

journal homepage: www.tjog-online.com

Original Article

Gene set-based integrative analysis of ovarian clear cell carcinoma

Chia-Ming Chang [a, b, c], Shih-Hwa Chiou [b, d], Ming-Jie Yang [a, c], Ming-Shyen Yen [a, c], Peng-Hui Wang [a, c, e, *]

[a] Department of Obstetrics and Gynecology, Taipei Veterans General Hospital, Taipei, Taiwan
[b] Institute of Oral Biology, National Yang-Ming University, Taipei, Taiwan
[c] Department of Obstetrics and Gynecology, National Yang-Ming University, Taipei, Taiwan
[d] Department of Medical Research, Taipei Veterans General Hospital, Taipei, Taiwan
[e] Department of Medical Research, China Medical University Hospital, Taichung, Taiwan

ARTICLE INFO

Article history:
Accepted 20 May 2016

Keywords:
clear cell adenocarcinoma
functionome
gene expression
integrative analysis

ABSTRACT

Objective: The pathogenesis of ovarian clear cell carcinoma is still poorly understood; therefore, we conducted a gene set-based analysis by integrating datasets downloaded from publicly available microarray gene expression databases to investigate the pathogenesis of clear cell carcinoma, which was based on the regularity of functions defined by gene ontology or canonical pathway databases.
Materials and Methods: The gene expression profiles of 80 clear cell carcinomas and 136 normal ovarian controls were downloaded from the National Center for Biotechnology Information Gene Expression Omnibus database. The gene expression profiles were converted to the gene set regularity (GSR) indexes computed using the modified differential rank conservation, an algorithm measuring the degree of gene expression ranking change in a gene set. Then the differences of GSR indexes between clear cell carcinomas and normal ovarian controls were analyzed.
Results: Machine learning can accurately recognize and classify the patterns of functional regularities containing the GSR indexes between the clear cell carcinomas and normal controls with an accuracy of 99.3%. The significant aberrations included oxidoreductase activity, binding, transport, channel activity, cell adhesion, immune response, chromosome assembly, and the deregulated signaling molecules, such as guanyl nucleotide exchange factors, phosphoinositide 3-kinase-activating kinase, receptor tyrosine kinase B, and protein tyrosine kinase.
Conclusion: Our pioneering works using the functionome, which was converted from microarray gene expression profiles for integrative analysis, showed a clear distinction of functional changes between the clear cell carcinomas and normal ovarian controls. This approach might provide a comprehensive view of the deregulated functions of clear cell carcinomas for further investigation.

Introduction

Ovarian carcinoma (OC), especially epithelial ovarian cancer, is one of the most lethal gynecological malignancies [1]. OC is a heterogeneous disease and consists of several molecularly and clinicopathologically distinct subtypes [2–4]. Clear cell carcinoma may be the most common secondary subtype, especially in Oriental countries such as Taiwan [5,6]. The prognosis of clear cell carcinoma is relatively poor, and the recurrence and 5-year survival rates were 27% and 60%, respectively [7]. The pathogenesis of clear cell carcinoma is unknown, but it is postulated to involve oxidative stress, genomic alterations, inflammatory processes, and estrogens [8,9].

Deoxyribonucleic acid (DNA) microarray gene expression is the primary tool to investigate the pathogenesis of various kinds of diseases, including clear cell carcinoma. The workflow of analyzing gene expression profiles usually consists of detecting the differentially expressed genes, and then mapping them to the gene ontology (GO) terms or signaling pathways for annotating the deregulated biological functions. However, this methodology focuses only on the statistically significant genes or pathways; the

* Corresponding author. Department of Obstetrics and Gynecology, Taipei Veterans General Hospital, 201, Section 2, Shih-Pai Road, Taipei 112, Taiwan.
E-mail addresses: phwang@vghtpe.gov.tw, phwang@ym.edu.tw (P.-H. Wang).

http://dx.doi.org/10.1016/j.tjog.2016.06.004

complete information about the regulation of the functions, for example, the functionome of clear cell carcinoma, is not provided.

Most of the microarray datasets investigating the pathogenesis of clear cell carcinoma were derived from a relatively small sample size. To overcome these limitations, we used a gene set based model to investigate the pathogenesis of clear cell carcinoma with the functionome. This model converts and quantizes the biological function defined by a gene set with the gene expression profiles downloaded from publicly available databases to a gene set regularity (GSR) index computed by the modified differential rank conservation (DIRAC) algorithm [10], which measured the matching degree of gene expression rankings in a given gene set between two different phenotypes, i.e., clear cell carcinomas and normal ovarian tissue controls in this study. This model utilized the gene set definitions from the GO term [11] and canonical pathways databases downloaded from the Molecular Signatures Database [12]. These two-gene set definitions collect relatively comprehensive biological functions, processes, or signaling pathways, so we used them to establish the human functionomes. The GO database contains 1454 gene sets, defining biological functions, processes, and cellular components. The canonical pathway database defines 1330 canonical signaling pathways, such as Kyoto Encyclopedia of Genes and Genomes (KEGG) and Reactome pathways. The pathogenesis of clear cell carcinoma was investigated with the functionomes using statistical methodologies.

Materials and methods

Microarray datasets, gene set definitions, and data processing

Gene expression microarray datasets were downloaded in the SOFT format from the National Center for Biotechnology Information (NCBI) Gene Expression Omnibus (GEO) database. The clear cell carcinoma and normal ovarian tissue control datasets were selected only when the samples originated from the ovarian tissue. The common genes, derived by intersecting of the genes from all datasets as well as the corresponding gene expression data, were used in this study. Datasets were discarded if the number of the common genes available was less than 8000 during cross-platform integration of these datasets. Gene sets were discarded if the number of gene elements in the gene set is less than three.

Computing GSR indexes by modified DIRAC

The algorithm for computing GSR indexes was modified from DIRAC, and the details are displayed in Figure 1. The GSR index measures the change of gene expression ranking between two phenotypes in a gene set. For this purpose, the GSR indexes of both the clear cell carcinoma and the normal control groups were computed by comparing the sample's gene expression ranking with a standard template, i.e., the baseline gene set ranking template derived from the most common gene expression ranking in a gene set among the entire normal ovarian tissue control samples. Then the subsequent analyses were carried out based on this same standard with the clear cell carcinoma and normal control GSR indexes. The baseline gene set raking template for each gene set is established by pairwise comparison between the expression levels of two genes for all possible combinations of gene pairs. Establishment of the baseline gene set expression-ranking template and measurement of GSR indexes were executed in (R code) environment; the code and the test datasets are available on the GitHub (https://github.com/carlzang/GSR-model.git).

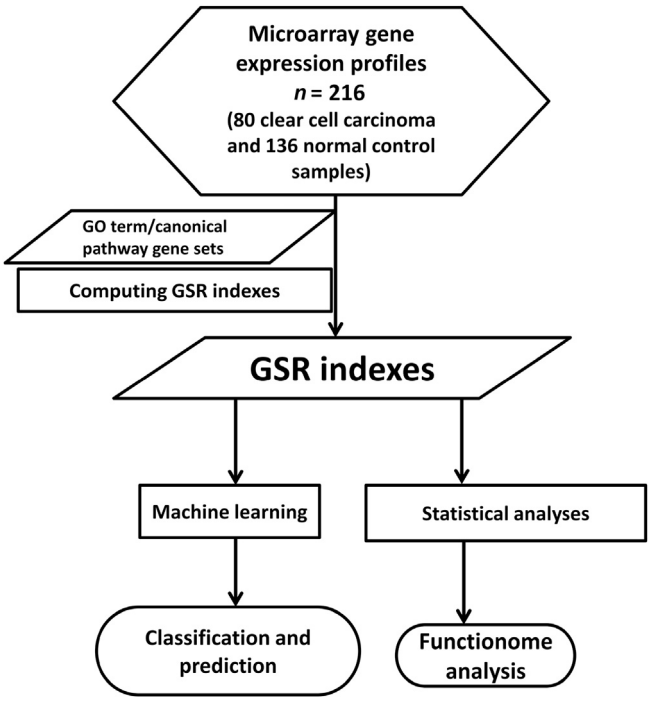

Figure 1. The gene set regularity (GSR) index was computed by converting the gene expression rankings of the clear cell carcinoma or normal ovarian control sample through each gene ontology (GO) term or canonical pathway gene set. Machine learning was trained to recognize the patterns consisting of GSR indexes, and then execute the binary (case-control) classifications. Functionome analysis was carried out by statistical methodologies to investigate the pathogenesis of clear cell carcinoma.

Statistical analysis

The differences between the clear cell carcinoma and control GSR indexes were tested using Mann–Whitney *U* test and corrected by multiple hypotheses using false discovery rate (Benjamini–Hochberg procedure). The significance level was set at $p < 0.001$.

Classification and prediction by machine learning

GSR index matrices computed through the GO term and canonical pathway gene sets were classified and predicted by "kernlab" [13], an R package for executing supporting vector machine (SVM) [14] with the setting of kernel = "rbfdot"(Radial Basis kernel "Gaussian"), type = "C-svc" (C classification). The performance of classification and prediction by SVM were measured by 5-fold cross-validation. The performance was assessed with the sensitivity, specificity, accuracy, and area under curve. The area under curve was computed using the R package "pROC" [15].

Establishment of GO tree

The tree of the deregulated GO terms was constructed and visualized by the RamiGO [16], an R package providing functions to interact with the AmiGO 2 web server (http://amigo2.berkeleybop.org/amigo) and retrieving GO trees.

Results

Sample information and means of the GSR indexes for clear cell carcinoma

DNA microarray gene expression datasets of the clear cell carcinoma samples were downloaded from the NCBI GEO database.

Table 1
Means and standard deviations of gene set regularity (GSR) indexes for the clear cell carcinoma (CCC) and control groups, and the performances of the binary (CCC vs. control group) classification and prediction by supporting vector machine with the GSR indexes computed through the gene ontology (GO) terms, canonical pathways, or combination of both (GO terms + canonical pathways).

Gene set	CCC	Control	SEN	SPE	Accuracy	AUC
GO terms	0.7400 (0.1180)	0.7727 (0.1329)	0.9888 (0.0234)	0.9965 (0.0109)	0.9930 (0.0112)	0.9921
Canonical pathways	0.7437 (0.1189)	0.7768 (0.1329)	0.9520 (0.0575)	1.0000 (0.0000)	0.9837 (0.01914)	0.9831
Both	0.7418 (0.1185)	0.7747 (0.1329)	0.9775 (0.0367)	0.9962 (0.0117)	0.9906 (0.0120)	0.9957

The sensitivities, specificities, accuracies, standard deviations, area under curve (AUC) were assessed by 5-fold cross-validation. Each measurement was computed by the cumulative results of repeating 10 times classifications and predictions.
Data presented as mean (standard deviation).
SEN = sensitivity; SPE = specificity.

The microarray gene expression datasets of clear cell carcinoma used in this study were GSE14764, GSE16570, GSE16574, GSE20565, GSE29450, GSE30161, GSE54807, GSE54809, GSE55512, GSE6008, and GSE63885, including five different microarray platforms: GPL96, GPL570, GPL7264, GPL6244, and GPL6947. The sample numbers were 80 clear cell carcinomas and 136 normal ovarian tissue controls. The GSR indexes ranged from 0 to 1, where 0 represents the most seriously deregulated function, whereas 1 represents the functional regulation in the clear cell carcinoma group that was completely unchanged in comparison with the most common gene expression ranking in the normal control population. The means of total GSR indexes computed through GO terms and canonical pathways for clear cell carcinomas were smaller than those of normal controls as displayed in Table 1, and the difference was statistically significant ($p < 0.001$). This indicated that clear cell carcinomas exhibited more deregulated functions defined by GO terms and canonical pathways than normal controls did.

Functional regulation patterns classified and predicted by machine learning

Machine learning can learn from data by building a model and recognizing patterns to make predictions. We trained SVM, a widely used machine-learning algorithm, to classify and predict the clear cell carcinoma and the normal control datasets with their functional regulation patterns consisting of the GSR indexes. The

Table 2
The top 40 most deregulated gene ontology terms of clear cell carcinoma ranked by the *p* values.

	Deregulated GO terms	p^*
1	Inositol or phosphatidylinositol phosphatase activity	1.33^{-16}
2	Cofactor transport	3.81^{-16}
3	Rho guanyl nucleotide exchange factor activity	3.81^{-16}
4	Small conjugating protein binding	6.59^{-16}
5	Ubiquitin binding	6.59^{-16}
6	Regulation of viral reproduction	9.88^{-16}
7	Vitamin transport	1.84^{-15}
8	Steroid hormone receptor binding	3.00^{-15}
9	Oxidoreductase activity acting on the CH-NH group of donors	2.20^{-14}
10	Histone deacetylase binding	3.09^{-14}
11	Protein tyrosine kinase activity	3.72^{-14}
12	Transmembrane receptor protein tyrosine kinase activity	5.46^{-14}
13	Carbohydrate biosynthetic process	7.43^{-14}
14	Insoluble fraction	7.59^{-14}
15	SH3 SH2 adaptor activity	2.03^{-13}
16	Regulation of muscle contraction	2.49^{-13}
17	Ras guanyl nucleotide exchange factor activity	3.14^{-13}
18	Negative regulation of cellular component organization and biogenesis	5.66^{-13}
19	Molecular adaptor activity	7.55^{-13}
20	Sarcomere	7.55^{-13}
21	Transmembrane receptor protein kinase activity	7.55^{-13}
22	Transferase activity transferring sulfur containing groups	1.43^{-12}
23	Aromatic compound metabolic process	1.86^{-12}
24	Embryonic development	3.32^{-12}
25	Neuropeptide signaling pathway	3.32^{-12}
26	Humoral immune response	3.58^{-12}
27	Isomerase activity	3.59^{-12}
28	Cytosolic part	3.81^{-12}
29	Nucleosome assembly	9.56^{-12}
30	Negative regulation of cell proliferation	9.59^{-12}
31	Oxygen binding	1.37^{-11}
32	Neutral amino acid transmembrane transporter activity	1.51^{-11}
33	Positive regulation of cell adhesion	1.56^{-11}
34	Microtubule	1.65^{-11}
35	Calcium channel activity	3.34^{-11}
36	Inward rectifier potassium channel activity	3.68^{-11}
37	Transmembrane receptor protein tyrosine kinase signaling pathway	5.63^{-11}
38	Auxiliary transport protein activity	7.45^{-11}
39	Oxidoreductase activity acting on sulfur group of donors	7.89^{-11}
40	Myofibril	8.50^{-11}

* Mann–Whitney *U* test and corrected by multiple hypotheses using false discovery rate.

results are shown in Table 1. The accuracy rates of binary classification (clear cell carcinomas vs. controls) were 99.30%, 98.37%, and 99.06% when computing through the GO terms, canonical pathways, or combination of both, respectively. SVM is a high-performance machine-learning algorithm, and this result revealed that the GSR indexes could provide sufficient and adequate information for SVM to perform accurate classification and prediction.

Deregulated GO terms and canonical pathways of clear cell carcinoma

The GSR index is derived from the extent of ranking change within a gene set defined by GO terms or canonical pathways between clear cell carcinomas and normal controls; thus, the GSR index represented the regulation of function defined by the gene set and could be used to investigate the pathogenesis by comparing the functional regulations between clear cell carcinomas and normal controls. Table 2 displays the top 40 most deregulated GO terms ranked by *p* values. The first deregulated GO term was "inositol or phosphatidylinositol phosphatase activity," followed by "cofactor transport" and "Rho guanyl nucleotide exchange factor activity." The deregulated GO terms shown in Table 2 can be summarized into the following categories: binding, transport, channel activity, cell adhesion, immune response, chromosome assembly, and deregulated signaling molecules, including guanyl nucleotide exchange factor, phosphatidylinositide 3-kinases (PI3Ks), as well as protein tyrosine kinase. Table 3 displays the top 40 deregulated canonical pathways ranked by *p* values. The first deregulated canonical pathway was "reactome downregulation of ErbB2, ErbB3 (receptor tyrosine kinase erbB-2, receptor tyrosine-protein kinase erbB-3) signaling," followed by "BioCarta MTA3 (metastasis associated 1 family, member 3) pathway" and "reactome negative regulation of the PI3K/activating kinase (AKT) network." It is interesting to find that the PI3K–AKT pathway appears repeatedly in Table 3.

Tree of deregulated GO terms for clear cell carcinoma

Because the GO terms are structured ontologies established according to the child–parent relationship, the deregulated GO gene set could be organized and displayed according to their GO hierarchies. Thus, the redundant GO terms could be identified and used to simplify the interpretation of results. The top 100 deregulated GO terms were utilized to establish the GO tree. The GO tree for clear cell carcinomas is displayed in detail in Figure 2, which shows the screenshot of the full GO tree and important deregulated GO terms. After being mapped to the GO tree, the related GO terms clustered together and revealed their hierarchies. Each cluster could be summarized by the common parental GO term. The deregulated GO terms in the figure could be divided into the following categories: metabolism, chromatin assembly, binding, binding, transport, cell cycle, cell adhesion, oxidoreductase activity, protein tyrosine kinase activity, and channel activity. The GO tree provided an intuitive way to view the structure of deregulated functions in the pathogenesis of clear cell carcinomas.

Discussion

Instead of detecting the differentially expressed genes, the study converted the microarray gene expression profiles of clear cell carcinomas to quantize biological functions through the gene sets defined by GO terms or canonical pathways, and then the pathogenesis of clear cell carcinoma was investigated by comparing the regularities of those functions between clear cell carcinomas and normal controls. In contrast to the "genome" analyzed with gene expression microarray, this model investigated "functionome" with the GSR indexes. By converting tens of thousands of gene expression profiles to approximately 1000 GSR indexes, this approach would diminish the data noise and simplify the subsequent analyses. Moreover, the GSR indexes are ordinal data derived from converting gene expression profiles to rankings; the ordinal data will encounter less bias than the gene expression levels during the integration of cross-platform profiles among different microarray gene expression datasets. In fact, with advanced technology and powerful computers, more detailed and comprehensive functional categories facilitated in KEGG and subsystem-based approach to high-throughput genome annotation (SEED) have been used for comparative genomics and as metagenomics tools to highlight functional features represented by KEGG automatic annotation server (KAAS) [17–19], MG-RAST (rapid annotations using subsystems technology server for metagenomic project) [20], and MEGAN (http://www-ab.informatik.uni-tuebingen.de/software/megan5/).

The functionome of clear cell carcinomas was composed of 1454 GO term-defined or 1330 canonical pathway-defined functions. Our result revealed that the functionomes could be recognized and accurately classified by the machine learning. This result indicated

Table 3
Top 40 deregulated canonical pathways of clear cell carcinoma ranked by *p* value.

	Deregulated canonical pathways	p^*
1	Reactome downregulation of ErbB2–ErbB3 signaling	3.20^{-17}
2	BioCarta MTA3 pathway	2.52^{-15}
3	Reactome negative regulation of the PI3K–AKT network	3.72^{-15}
4	PID integrin 5 pathway	2.30^{-14}
5	PID RET pathway	1.33^{-13}
6	Reactome phospholipase C mediated cascade	1.33^{-13}
7	PID NF-kappaB canonical pathway	1.49^{-13}
8	Reactome PERK regulated gene expression	5.42^{-13}
9	Reactome FGFR ligand binding and activation	8.14^{-13}
10	BioCarta myosin pathway	1.33^{-12}
11	KEGG inositol phosphate metabolism	2.01^{-12}
12	Reactome ethanol oxidation	2.01^{-12}
13	Reactome PI 3K cascade	2.55^{-12}
14	Reactome regulation of RHEB GTPase activity by AMPK	2.80^{-12}
15	Reactome beta defensins	3.02^{-12}
16	PID RAC1 REG pathway	3.05^{-12}
17	Reactome GPVI mediated activation cascade	4.69^{-12}
18	Reactome insulin receptor signaling cascade	4.69^{-12}
19	Reactome PI3K cascade	4.69^{-12}
20	KEGG gap junction	4.89^{-12}
21	KEGG phosphatidylinositol signaling system	4.89^{-12}
22	KEGG tryptophan metabolism	4.89^{-12}
23	Reactome activation of genes by ATF4	6.63^{-12}
24	Reactome mRNA decay by 3 to 5 exoribonuclease	7.08^{-12}
25	BioCarta PAR1 pathway	8.15^{-12}
26	Reactome common pathway	1.07^{-11}
27	Reactome signaling by Robo receptor	1.53^{-11}
28	Reactome phase 1 functionalization of compounds	1.65^{-11}
29	Reactome CD28 dependent PI3K Akt signaling	1.71^{-11}
30	KEGG pathogenic Escherichia coli infection	2.41^{-11}
31	Reactome G0 and early G1	3.68^{-11}
32	Reactome PI3K events in ERBB2 signaling	3.68^{-11}
33	Reactome downstream signaling of activated FGFR	3.91^{-11}
34	PID integrin 2 pathway	4.45^{-11}
35	KEGG butanoate metabolism	6.39^{-11}
36	KEGG steroid hormone biosynthesis	6.39^{-11}
37	BioCarta RAC1 pathway	6.59^{-11}
38	PID A6B1 A6B4 integrin pathway	6.68^{-11}
39	Reactome signaling by NODAL	7.40^{-11}
40	Reactome signaling by FGFR	8.19^{-11}

* Mann–Whitney *U* test and corrected by multiple hypotheses using false discovery rate.
AMPK = adenosine monophosphate-activated protein kinase; FGFR = fibroblast growth factor receptor; KEGG = Kyoto Encyclopedia of Genes and Genomes; PI3K = phosphatidylinositide 3-kinase.

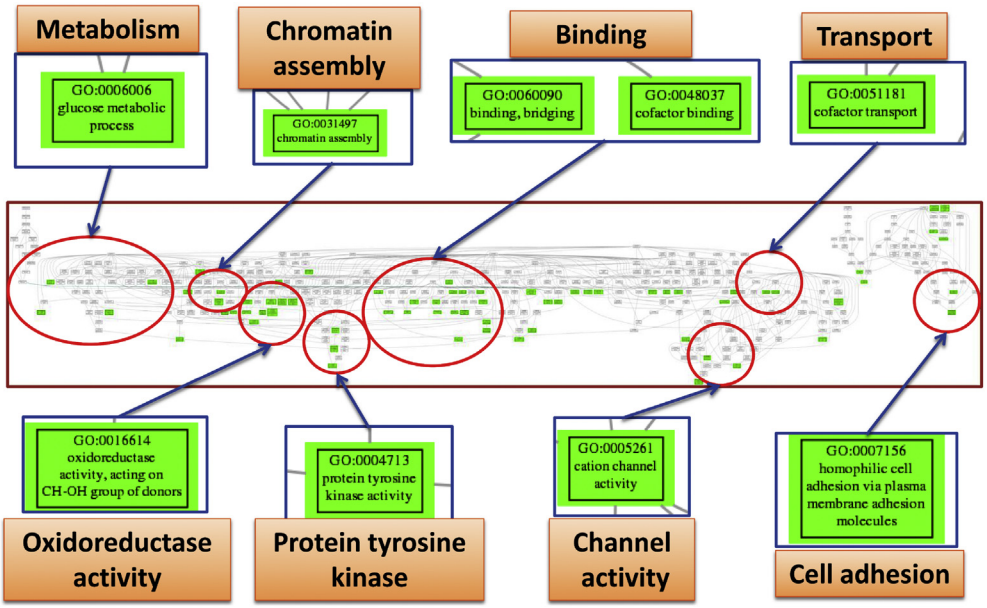

Figure 2. Screenshot of the full clear cell carcinoma gene ontology (GO) tree in the middle. The important GO terms (green boxes) in each cluster are magnified to display the details, and each cluster is labeled by their common parental GO terms (orange boxes).

the practicability of molecular classification with the functionome. Among the deregulated GO terms shown in Table 2, the most deregulated GO term, "inositol or phosphatidylinositol phosphatase activity," revealed that PI3K played a key step in the pathogenesis of clear cell carcinoma. Matsuzaki et al [21] had published an article entitled "Potential targets for ovarian clear cell carcinoma" and also showed the important role of PI3K–AKT–mTOR (mammalian target of rapamycin) signaling pathway of ovarian clear cell carcinoma on the platinum resistance. In addition, PI3K/AKT pathway activation may be also related to ovarian clear cell carcinoma development [22], and account for 40% of ovarian cancers [23]. The signals from the receptor tyrosine kinase (RTK) transduced to the PI3K–AKT pathway and aberrantly regulated cell proliferation, inhibition of apoptosis, and cell adhesion. These aberrations led to abnormal chromatin assembly and eventually the carcinogenesis of clear cell carcinoma. The deregulated canonical pathways shown in Table 3 provided the additional evidence supporting these findings. The PI3K–AKT pathway was the third most significantly deregulated gene set in the canonical pathways database. All supported the validity of our current approach.

ErbB2 was the most significantly deregulated canonical pathways in Table 3; it is expressed in OCs ranging from 20% to 30% [24] and is a member of the epidermal growth factor receptor (EGFR) family. Sereni et al [25] found that the expression of EGFR Y1068 and human epidermal growth factor receptor(HER)/ErbB2 Y1248 was significantly increased and/or activated in clear cell carcinomas of the ovary. By contrast, this significant increase in the expression/activation level of EGFR Y1068 and HER/ErbN2 Y1248 was only found in ovarian clear cell carcinoma, whereas all other histosubtypes of ovarian cancers, such as high-grade serous carcinoma, endometrioid carcinoma, and mixed types, showed the significant downregulation of both EGFR Y1068 and HER/ErbB2 Y1248 [25]. In fact, ErbB2 can activate the PI3K–AKT pathway; therefore, it is reasonable to find the results of upregulated expression of both EGFR Y1068 and HER/ErbB2 Y1248. This hypothesis was supported by the current study, because we found the 31st deregulated pathway "Reactome PI3K events in ErbB2 signaling," revealing the interaction between the two pathways.

The second important deregulated GO term was "cofactor transport," and the fourth was "small conjugating protein binding" deregulated GO terms, suggesting the importance of cofactors for the carcinogenesis of clear cell carcinoma, such as the third "Rho guanyl nucleotide exchange factors" and the 17th "ras guanyl nucleotide exchange factors"—two proteins regulating the switches of ras activation or deactivation. Recently, Takai et al [26] found the crosstalk between PI3K and ras pathways in human ovarian clear cell carcinoma, which was mediated by protein phosphatase 2A, suggesting that aberration of the ras system was also important in the development of clear cell carcinoma.

In conclusion, with the microarray gene expression datasets downloaded from publicly available databases, the functionome analysis provided a more comprehensive view of the pathogenesis of clear cell carcinoma. Clear cell carcinomas were involved in the aberrations of oxidoreductase activity, cell adhesion, channel activity, transport and metabolism, and the aberrant signaling cascades including RTK, ras pathway, PI3K–AKT, and ErbB pathways. This study might be the first integrative analysis investigating the pathogenesis of ovarian clear cell carcinoma; the results not only showed the aberrant pathways being compatible with current knowledge, but also provided a more comprehensive picture of the deregulated functions for this disease.

Conflicts of interest

The authors have no conflicts of interest relevant to this article.

Acknowledgments

This work was supported by grants from the Ministry of Science and Technology, Executive Yuan (MOST 103-2314-B-010-043-MY3), and Taipei Veterans General Hospital (V102C-141; V103C-112: V104C-095; and V105C-096). The funders had no role in study design, data collection and analysis, decision to publish, or preparation of the manuscript. No additional external funding was received for this study. We thank the Medical Science and

Technology Building of Taipei Veterans General Hospital for providing experimental space and facilities.

References

[1] Chang WH, Wang KC, Lee WL, Huang N, Chou YJ, Feng RC, et al. Endometriosis and the subsequent risk of epithelial ovarian cancer. Taiwan J Obstet Gynecol 2014;53:530–5.

[2] Wang PH, Sun HD, Lin H, Wang KL, Liou WS, Hung YC, et al. Outcome of patients with recurrent adult-type granulosa cell tumors—a Taiwanese Gynecology Group (TGOG) study. Taiwan J Obstet Gynecol 2015;54:253–9.

[3] Chao A, Lai CH, Chen HC, Lin CY, Tsai CL, Tang YH, et al. Serum microRNAs in clear cell carcinoma of the ovary. Taiwan J Obstet Gynecol 2014;53:536–41.

[4] Sun HD, Hsiao SM, Wen KC, Wang PH. Isolated Krukenberg tumor in pregnancy. Taiwan J Obstet Gynecol 2015;54:211–2.

[5] Lee WL, Chang WH, Wang KC, Guo CY, Chou YJ, Huang N, et al. The risk of epithelial ovarian cancer of women with endometriosis may be varied greatly if diagnostic criteria are different: A nationwide population-based cohort study. Medicine (Baltimore) 2015;94:e1633.

[6] Wang KC, Chang WH, Lee WL, Huang N, Huang HY, Yen MS, et al. An increased risk of epithelial ovarian cancer in Taiwanese women with a new surgicopathological diagnosis of endometriosis. BMC Cancer 2014;14:831.

[7] Sugiyama T, Kamura T, Kigawa J, Terakawa N, Kikuchi Y, Kita T, et al. Clinical characteristics of clear cell carcinoma of the ovary: a distinct histologic type with poor prognosis and resistance to platinum-based chemotherapy. Cancer 2000;88:2584–9.

[8] Yamada Y, Shigetomi H, Onogi A, Haruta S, Kawaguchi R, Yoshida S, et al. Redox-active iron-induced oxidative stress in the pathogenesis of clear cell carcinoma of the ovary. Int J Gynecol Cancer 2011;7:1200–7.

[9] Huang BS, Lee WL, Wang PH. The slowing down of renal deterioration but acceleration of cardiac hypertrophy—is estrogen receptor α a hero or villain? Am J Physiol Renal Physiol 2014;307:F1352–4.

[10] Eddy JA, Hood L, Price ND, Geman D. Identifying tightly regulated and variably expressed networks by Differential Rank Conservation (DIRAC). PLoS Comput Biol 2010;6:e1000792.

[11] Ashburner M, Ball CA, Blake JA, Botstein D, Butler H, Cherry JM, et al. Gene ontology: tool for the unification of biology. The Gene Ontology Consortium. Nat Genet 2000;25:25–9.

[12] Subramanian A, Tamayo P, Mootha VK, Mukherjee S, Ebert BL, Gillette MA, et al. Gene set enrichment analysis: a knowledge-based approach for interpreting genome-wide expression profiles. Proc Natl Acad Sci U S A 2005;102:15545–50.

[13] Karatzoglou A, Smola A, Hornik K. Kernel-based machine learning lab. Version 0.9-24 https://cran.r-project.org/web/packages/kernlab/kernlab.pdf

[14] Robin X, Turck N, Hainard A, Tiberti N, Lisacek F, Sanchez JC, et al. pROC: an open-source package for R and S+ to analyze and compare ROC curves. BMC Bioinformatics 2011;12:77.

[15] Schröder MS, Gusenleitner D, Quackenbush J, Culhane AC, Haibe-Kains B. RamiGO: an R/Bioconductor package providing an AmiGO visualize interface. Bioinformatics 2013;29:666–8.

[16] Cortes C, Vapnik V. Support-vector networks. Mach Learn 1995;20:273.

[17] Kanehisa M, Goto S. KEGG: Kyoto Encyclopedia of Genes and Genomes. Nucleic Acids Res 2000;28:27–30.

[18] Overbeek R, Begley T, Butler RM, Choudhuri JV, Chuang HY, Cohoon M, et al. The subsystems approach to genome annotation and its use in the project to annotate 1000 genomes. Nucleic Acids Res 2005;33:5691–702.

[19] Moriya Y, Itoh M, Okuda S, Yoshizawa A, Kanehisa M. KAAS: an automatic genome annotation and pathway reconstruction server. Nucleic Acids Res 2007;35:W182–5.

[20] Meyer F, Paarmann D, D'Souza M, Olson R, Glass EM, Kubal M, et al. The metagenomics RAST server—a public resource for the automatic phylogenetic and functional analysis of metagenomes. BMC Bioinformatics 2008;9:386.

[21] Matsuzaki S, Yoshino K, Ueda Y, Matsuzaki S, Kakuda M, Okazawa A, et al. Potential targets for ovarian clear cell carcinoma: a review of updates and future perspectives. Cancer Cell Int 2015;15:117.

[22] Huang HN, Lin MC, Huang WC, Chiang YC, Kuo KT. Loss of ARID1A expression and its relationship with PI3K–Akt pathway alterations and ZNF217 amplification in ovarian clear cell carcinoma. Mod Pathol 2014;27:983–90.

[23] Hashiguchi Y, Tsuda H, Inoue T, Berkowitz RS, Mok SC. PTEN expression in clear cell adenocarcinoma of the ovary. Gynecol Oncol 2006;101:71–5.

[24] Leary JA, Edwards BG, Houghton CR, Kefford RF, Friedlander ML. Amplification of HER-2/neu oncogene in human ovarian cancer. Int J Gynecol Cancer 1992;2:291–4.

[25] Sereni MI, Baldelli E, Gambara G, Deng J, Zanotti L, Bandiera E, et al. Functional characterization of epithelial ovarian cancer histotypes by drug target based protein signaling activation mapping: implications for personalized cancer therapy. Proteomics 2015;15:365–73.

[26] Takai M, Nakagawa T, Tanabe A, Terai Y, Ohmichi M, Asahi M. Crosstalk between PI3K and Ras pathways via protein phosphatase 2A in human ovarian clear cell carcinoma. Cancer Biol Ther 2015;16:325–35.